ACS ORGANIC & INORGANIC Au
AN OPEN ACCESS JOURNAL OF THE AMERICAN CHEMICAL SOCIETY

pubs.acs.org/orginorgau

Article

Photomicellar Catalyzed Synthesis of Amides from Isocyanides: Optimization, Scope, and NMR Studies of Photocatalyst/Surfactant Interactions

Rolando Cannalire,[§] Federica Santoro,[§] Camilla Russo, Giulia Graziani, Gian Cesare Tron, Alfonso Carotenuto,* Diego Brancaccio,* and Mariateresa Giustiniano*

Cite This: *ACS Org. Inorg. Au* 2022, 2, 66−74

Read Online

ACCESS | Metrics & More | Article Recommendations | Supporting Information

ABSTRACT: The merging of micellar and photoredox catalysis represents a key issue to promote "in water" photochemical transformations. A photomicellar catalyzed synthesis of amides from *N*-methyl-*N*-alkyl aromatic amines and both aliphatic and aromatic isocyanides is herein presented. The mild reaction conditions enabled a wide substrate scope and a good functional groups tolerance, as further shown in the late-stage functionalization of complex bioactive scaffolds. Furthermore, solution 1D and 2D NMR experiments performed, for the first time, in the presence of paramagnetic probes enabled the study of the reaction environment at the atomic level along with the localization of the photocatalyst with respect to the micelles, thus providing experimental data to drive the identification of optimum photocatalyst/surfactant pairing.

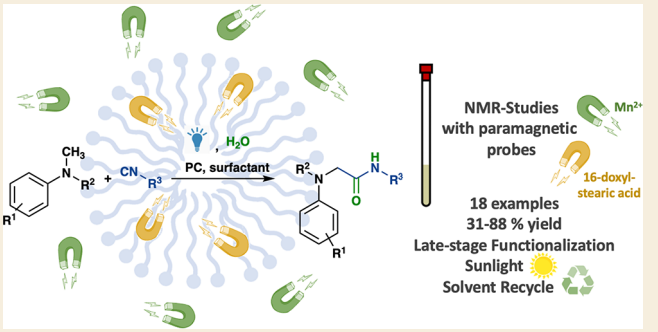

KEYWORDS: *photocatalysis, micellar catalysis, isocyanides, amides, NMR probes*

INTRODUCTION

Aqueous micellar catalysis, beyond "on water" and "with water" reactions,[1−4] has been established as a huge opportunity to perform *in water* reactions, thus drawing synthetic organic chemistry procedures closer to Nature's mild reaction conditions.[5−7] The aggregation of surfactants to micellar nanoreactors offers indeed the possibility of mimicking enzymes' hydrophobic pockets, which provide suitable reaction vessels for lipophilic substrates.

By overcoming the need for large amounts of organic solvents, while preserving their efficiency and selectivity in promoting organic transformations, micellar catalysis enables the reduction of organic waste along with the prevention of water stream contamination arising from the use of water-miscible solvents.[8] Despite the far-reaching advances in the application of micellar catalysis to a wide range of key synthetic transformations (spanning from condensations, oxidations, deprotections, multicomponent reactions, C−C and C-heteroatom bond-forming processes, and even metal-catalyzed cross-couplings),[79] very few reports about visible-light-promoted reactivities of radical precursors in water are so far available.[10−12] Water has been indeed mostly reported as a cosolvent, in order to achieve complete dissolution of reactants/reagents for homogeneous conditions or as the oxygen source.[13−15] Recently, Lipshutz developed an amphoteric polyethylene glycol ubiquinol succinate (PQS)-attached photocatalyst able to self-aggregate in water into nanomicelles, whereas the covalently bound Ir complex promotes, upon visible light excitation, the formation of open shell species from suitable precursors[16] (Figure 1a). If substantial advantages are associated with this catalytic system, such as the possibility to recycle the metal catalyst several times, the necessity of a covalent functionalization of the surfactants to introduce the active photocatalytic moiety could limit a broad application of this approach. This observation is even more relevant when new chemical transformations are involved if considering the necessity to screen different photocatalysts endowed with different redox potentials, i.e., either stronger or poorer oxidants/reductants, as well as different surfactants to achieve optimum reaction conditions.

To this end, the commercial availability of a wide range of surfactants covalently modified with photoredox active catalysts would expedite the spreading of micellar systems as reaction media in visible-light-triggered transformations. Meanwhile, with the hope that such an array of photoactive

Received: September 27, 2021
Revised: October 26, 2021
Accepted: October 26, 2021
Published: November 11, 2021

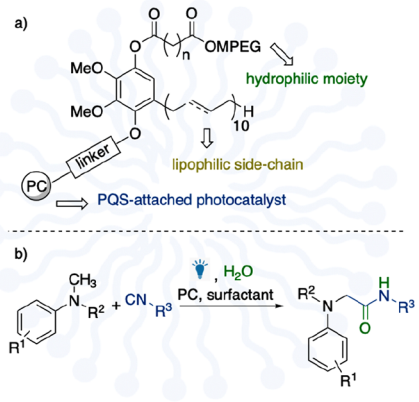

Figure 1. (a) Lipshutz PQS-attached photocatalyst. (b) *In water* formation of amides from isocyanides developed herein.

micelles will be soon available, we wondered if the switch from organic solvents to aqueous micellar solutions could be feasible, at least for those transformations involving water either as a cosolvent or a substrate. It is worth noting that, in the 1980s, the influence of micelles on photochemical reactivity was of great interest due to the possibility of modulating the reaction outcome via cage, preorientational, polarity, and counterion effects.[17,18] In light of these considerations and following our interests in isocyanides involving visible-light-phototriggered processes,[19,20] we sought to investigate the opportunities and the challenges of synthesizing amides from such an intriguing class of organic compounds and *N*-methyl-*N*-alkyl aromatic amines in water (Figure 1b).

RESULTS AND DISCUSSION

The model reaction was reported in 2013 by Rueping et al. and required acetonitrile as the optimum solvent system, whereas water was used as a substrate in a 10 equiv amount.[21,22] A preliminary test reaction involving *N*,*N*-dimethylaniline **1** and toluenesulfonylmethyl isocyanide (TosMIC) **2**, performed in 2% TPGS-750-M (0.15 M) at room temperature and under irradiation with 16 W blue light-emitting diodes (LEDs) for 48 h, gave the desired product **3** in a fair 30% yield, proving that a water-based solvent system could be feasible for this transformation (Table 1, entry 2) (as a reference, **3** was obtained in 70% yield when the reaction was performed in acetonitrile according to literature conditions, entry 1). To identify optimum *in water* reaction conditions, we performed the reaction in the presence of different micellar media (Figure 2) and different photoredox catalysts and by changing temperature, light source potency, and equivalents of starting materials **1** and **2** (Table 1).

Although irradiation with 30 W blue LEDs slightly increased the yield (entry 3), the beneficial micellar effect was apparent if compared with the reaction performed in pure water (entry 4). An increase of the reaction temperature to ∼50 °C (fan switched off) led to detrimental results both in TPGS-750-M and in pure water (entries 5 and 6), as well as the addition of Na_2CO_3 as a base (entry 7). Interestingly, an increment of *N*,*N*-dimethylaniline equivalents from 1 to 2 together with a lower amount of isocyanide **2** (1 equiv) led to a good 68% yield (entry 8). Decreasing **1** to 1.5 equiv was detrimental (entry 9), although, again, the micellar medium was shown to be key for the success of the reaction (entry 10). A further

Table 1. Optimization of Reaction Conditions

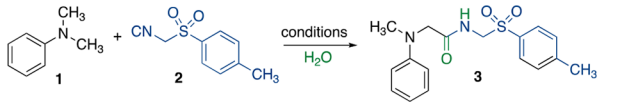

Entry	Eq. 1	Eq. 2	PC (mol%)	Solvent (0.15 M)	T	Watt	Yield %
1	1	1.5	$[Ir(ppy)_2bpy]PF_6$ (1)	MeCN/H_2O (10 eq)	rt	16	70 (litt 70)
2	1	1.5	$[Ir(ppy)_2bpy]PF_6$ (1)	2% TPGS-750-M	rt	16	30[b]
3	1	1.5	$[Ir(ppy)_2bpy]PF_6$ (1)	2% TPGS-750-M	rt	30	40[b]
4	1	1.5	$[Ir(ppy)_2bpy]PF_6$ (1)	H_2O	rt	30	20[b]
5	1	1.5	$[Ir(ppy)_2bpy]PF_6$ (1)	2% TPGS-750-M	50°C	30	15[b]
6	1	1.5	$[Ir(ppy)_2bpy]PF_6$ (1)	H_2O	50°C	30	12[b]
7[a]	1	1.5	$[Ir(ppy)_2bpy]PF_6$ (1)	2% TPGS-750-M	rt	30	ND
8	2	1	$[Ir(ppy)_2bpy]PF_6$ (1)	2% TPGS-750-M	rt	30	68 (50[b])
9	1.5	1	$[Ir(ppy)_2bpy]PF_6$ (1)	2% TPGS-750-M	rt	30	38[b]
10	2	1	$[Ir(ppy)_2bpy]PF_6$ (1)	H_2O	rt	30	22[b]
11	2	1	fac-$Ir(ppy)_3$ (1)	2% TPGS-750-M	rt	30	25[b]
12	2	1	$Ru(bpy)_3(PF_6)_2$	2% TPGS-750-M	rt	30	6.5[b]
13	2	1	Rose Bengal (1)	2% TPGS-750-M	rt	30	20[b]
14	2	1	Eosin Y (1)	2% TPGS-750-M	rt	30	17[b]
15	2	1	$[Mes\text{-}Acr]BF_4$ (1)	2% TPGS-750-M	rt	30	7[b]
16	2	1	Eosin Y (5)	2% TPGS-750-M	rt	30	20[b]
17	2	1	$[Ir(ppy)_2bpy]PF_6$ (1)	1% TPGS-750-M	rt	30	12[b]
18	2	1	$[Ir(ppy)_2bpy]PF_6$ (1)	2% SPGS-550-M	rt	30	33[b]
19	2	1	$[Ir(ppy)_2bpy]PF_6$ (1)	5% TPGS-750-M	rt	30	32[b]
20	2	1	$[Ir(ppy)_2bpy]PF_6$ (1)	2% Triton X-100	rt	30	31[b]
21	2	1	Eosin Y (5)	2% Triton X-100	rt	30	30[b]
22	2	1	$[Ir(ppy)_2bpy]PF_6$ (1)	2% CTAC	rt	30	15[b]
23	2	1	Eosin Y (5)	2% CTAC	rt	30	30[b]
24	2	1	$[Ir(ppy)_2bpy]PF_6$ (1)	2% SDS	rt	30	75(64[b])
25	2	1	Eosin Y (5)	2% SDS	rt	30	18[b]
26	2	1	$[Ir(ppy)_2bpy]PF_6$ (0.5)	2% SDS	rt	30	25[b]

[a]in presence of Na_2CO_3 (1 eq.); [b]NMR yield.

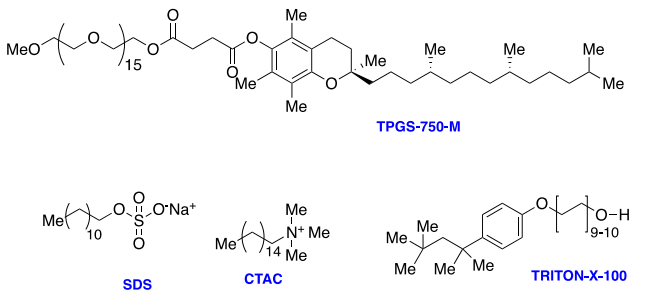

Figure 2. Structures of the surfactants tested.

screening of both metal-based and organic photocatalysts did not produce better results (entries 11−16), whereas a survey of different micellar media (entries 17−24) resulted in the identification of a 2% solution of sodium dodecyl sulfate (SDS) as the best solvent system (entry 24), enabling a yield comparable to that of acetonitrile (entry 1).

When these reaction conditions were applied to a 10-fold mmol scale (3 mmol), they proved to still be able to provide the desired product, although in a moderate 20% yield. Finally, further attempts to use an organic photocatalyst (entry 25) as well as reducing the catalyst loading (entry 26) were unproductive. On the basis of the reaction mechanism proposed by Rueping et al.,[21] the presence of molecular oxygen (the reaction was performed open flask) was key to provide an electron donor able to regenerate the iridium photocatalyst.

With the aim of proving the generality of these *in water* optimum reaction conditions, the substrate scope was investigated by reacting *N*,*N*-dimethylaniline **1** with different aliphatic isocyanides (yields in parentheses refer to the reaction performed in acetonitrile as reported in ref 21; Figure 3). Both primary (**4**−**6**, Figure 3) and secondary (**7**, Figure 3) isocyanides were competent substrates with yields spanning from 55 to 75%. In addition, less nucleophilic aromatic isocyanides, regardless the presence of either electron-with-

https://doi.org/10.1021/acsorginorgau.1c00028
ACS Org. Inorg. Au 2022, 2, 66−74

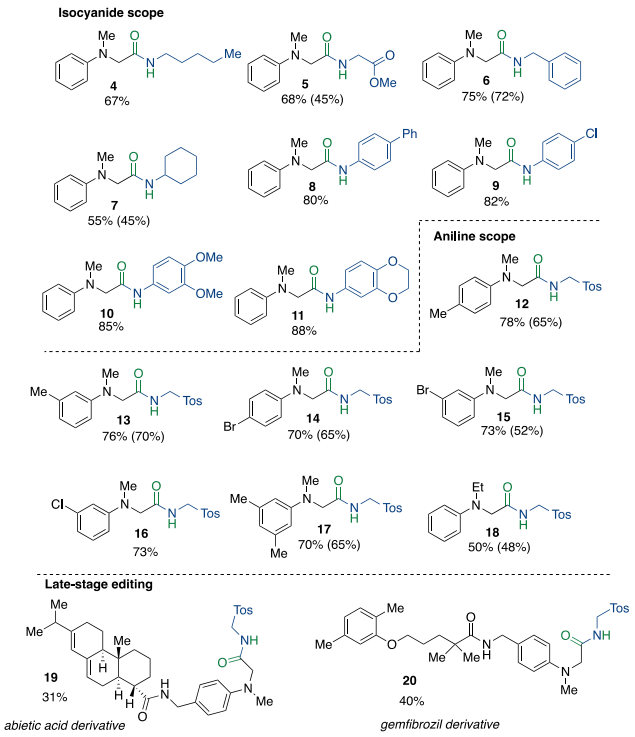

Figure 3. Reaction scope (standard reaction conditions as in Table 1, entry 24, performed on a 0.3 mmol scale; yields in parentheses refer to the reaction performed in acetonitrile as reported in ref 21).

drawing (**8** and **9**, Figure 3) or electron-donating (**10** and **11**, Figure 3) substituents, smoothly afforded the corresponding amides in 80−88% yields.

Similarly, the aromatic amine scope was good, with yields close to or higher than those obtained when using acetonitrile both for electron-poor (**14**−**16**, Figure 3) and electron-rich (**12**, **13**, **17**, Figure 3) anilines. Finally, nonsymmetrical *N*-ethyl-*N*-methylaniline regioselectively afforded amide **18** in a good 50% yield (Figure 3). Noteworthy, late-stage functionalization of abietic acid and gemfibrozil-derived *N*,*N*-dimethylanilines was accomplished in 31 and 40% yields, respectively. To further demonstrate the robustness of this methodology, the reaction was performed under sunlight irradiation, providing the target compound **3** in a good 60% yield (Scheme 1).

Additionally, the micellar aqueous mixture can be recycled with no or slight change in the yield (Scheme 1).

To investigate whether a rational approach for selecting the best performing photocatalyst/surfactant pairs could be feasible, the interactions occurring between the photocatalyst and SDS and cetyltrimethylammonium chloride (CTAC) 2% solutions (i.e., the most and the least efficient micellar systems) were investigated at the atomic level via solution NMR techniques.[23]

1D ^{1}H NMR spectra of $[Ir(ppy)_2bpy]PF_6$ in pure water and in the presence of micelles (Figure S1, Supporting Information) were very different, indicating that the interaction between the catalyst and the micelles occurred in both cases. While the spectrum of the catalyst in pure water showed low intensity and broad signals (Figure S1a, Supporting Information), probably due to its poor solubility and, as a consequence, to aggregation phenomena, both the proton spectra acquired in SDS and CTAC 2% solutions showed

Scheme 1. (a) Natural Sunlight Induced Reaction and (b) Recycle Performed by Introducing All Components to the Aqueous Reaction Mixture from the Previous Reaction after Extraction with EtOAc

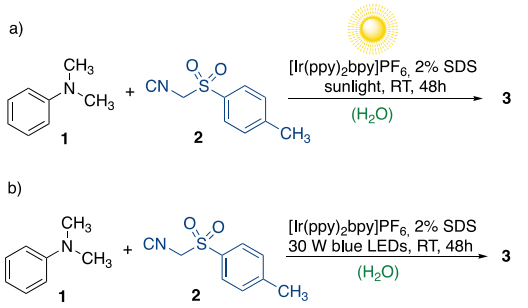

Initial reaction	1st recycle	2nd recycle	3rd recycle
75%	75%	75%	60%

narrow and well-resolved signals (Figure S1b,c, Supporting Information), being similar to each other and similar to that obtained in organic solvents (e.g., CD_2Cl_2).[24]

Complete assignment of the proton signals of $[Ir(ppy)_2bpy]PF_6$ in the presence of micelles was achieved via the analysis of 2D ^{1}H−^{1}H COSY,[25,26] TOCSY,[27] and NOESY[28] spectra (Tables S1 and S2, Supporting Information). Furthermore, the localization of $[Ir(ppy)_2bpy]PF_6$ relative to the surface and the interior of SDS or CTAC micelles was studied using paramagnetic probes: 16-doxyl-stearic acid (16-doxyl) and Mn^{2+}. It is well-known, indeed, that unpaired electrons could lead to dramatically accelerated longitudinal and transverse relaxation rates of protons in spatial proximity via highly efficient spin and electron relaxation.[29] Therefore, these paramagnetic probes were expected to cause the broadening of the NMR signals and a decrease in resonance intensities either for a molecule outside the micelle (Mn^{2+}) or deeply buried in the micelle (16-doxyl).[30,31]

Accordingly, ^{1}H NMR spectra of $[Ir(ppy)_2bpy]PF_6$, in micellar solutions, in the presence of increasing concentrations of the spin-labels (Figure 4a−h and a′−h′), with all other conditions kept constant, were recorded.

The signal intensities of $[Ir(ppy)_2bpy]PF_6$ in SDS 2% solution showed significant reduction of all signals after the addition of both the Mn^{2+} and the 16-doxyl at the highest concentrations (Figure 4f−h and g′,h′).

This result suggested that the catalyst is, on average, positioned on the micelle surface and can flip from the outer to inner part of it so that it can feel both the external (Mn^{2+}) and internal (16-doxyl) paramagnetic effects. More detailed investigation revealed that protons H4/H7 and H3/H8 were the most affected by Mn^{2+}, whereas protons H15/H26, H19/H30, and H18/H29 were the most affected by 16-doxyl even at the lower concentration used for these paramagnetic probes (Figure 5).

Considering the same catalyst $[Ir(ppy)_2bpy]PF_6$ in CTAC micelles (Figure 6a−h and a′−h′), a generalized reduction of the signals' intensity was observed upon the addition of 16-doxyl (Figure 5d′−h′), while the addition of Mn^{2+} reduced the signal intensity of 30% at most (Figure 6b−h). These findings demonstrated that $[Ir(ppy)_2bpy]PF_6$ tended to be deeply inserted in CTAC micelles, probably because of the electronic repulsion between the positively charged metal center of the

https://doi.org/10.1021/acsorginorgau.1c00028
ACS Org. Inorg. Au 2022, 2, 66−74

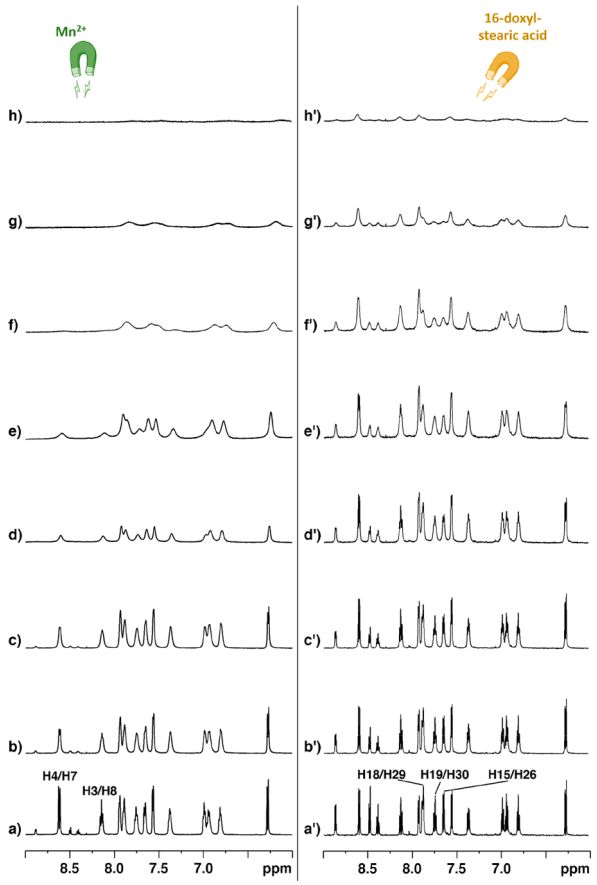

Figure 4. ^{1}H NMR spectra of [Ir(ppy)$_2$bpy]PF$_6$, in SDS 2% solution (a,a′) and in the presence of 0.1 mM (b,b′), 0.2 mM (c,c′), 0.5 mM (d,d′), 1.0 mM (e,e′), 2.0 mM (f,f′), 3.0 mM (g,g′), and 5.0 mM (h,h′) of Mn^{2+} (left) and 16-doxylstearic acid (right) probes.

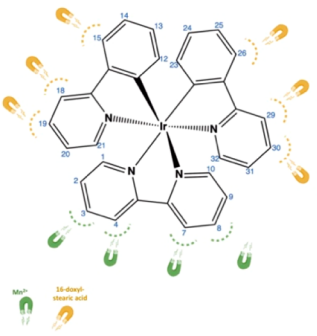

Figure 5. Schematic representation of most affected protons of [Ir(ppy)$_2$bpy]PF$_6$ by Mn^{2+} (green) and 16-doxylstearic acid (yellow) in SDS 2% solution.

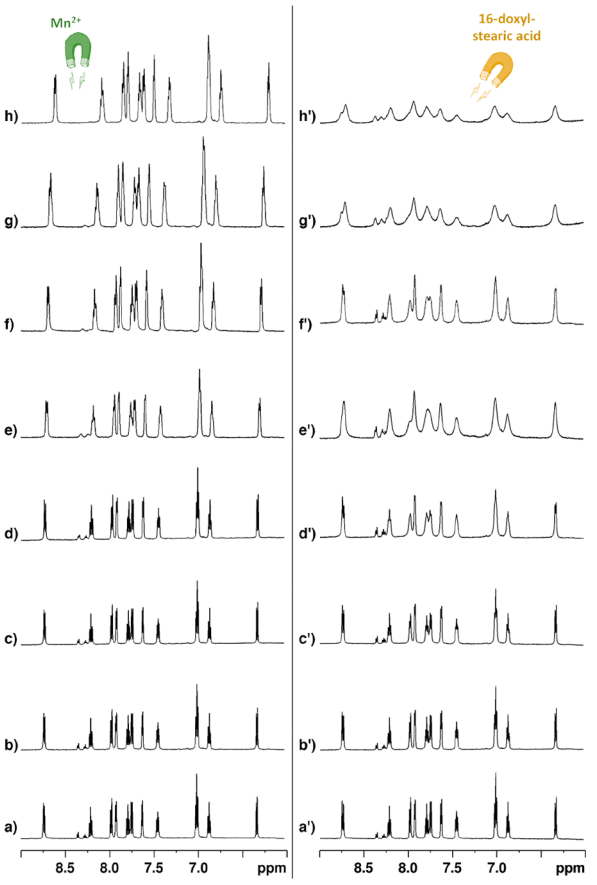

Figure 6. ^{1}H NMR spectra of [Ir(ppy)$_2$bpy]PF$_6$, in CTAC 2% solution (a,a′) and in the presence of 0.1 mM (b,b′), 0.2 mM (c,c′), 0.5 mM (d,d′), 1.0 mM (e,e′), 2.0 mM (f,f′), 3.0 mM (g,g′), and 5.0 mM (h,h′) of Mn^{2+} (left) and 16-doxylstearic acid (right) probes.

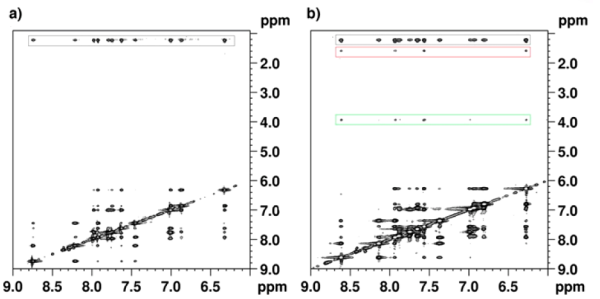

Figure 7. ^{1}H−^{1}H 2D NOESY spectra of [Ir(ppy)$_2$bpy]PF$_6$ in CTAC (a) and (b) SDS 2% solutions. Different signal strips are evidenced as boxes: black, main chain CH_2; green, αCH_2; red, βCH_2.

photocatalyst and the CTAC quaternary ammonium head. To further investigate the catalyst/micelle relative orientation, we acquired NOESY[28] spectra of the catalyst together with (not deuterated) SDS and CTAC 2% solutions (Figure 7).

As shown in Figure 7a, NOE cross-peaks corresponding to intermolecular contacts are observable in the [Ir(ppy)$_2$bpy]-PF$_6$−CTAC system only from the main chain CH_2 of CTAC with all the catalyst protons, thus confirming that [Ir-(ppy)$_2$bpy]PF$_6$ is deeply buried into these micelles. Considering the [Ir(ppy)$_2$bpy]PF$_6$/SDS system (Figure 7b), cross-peaks attributable to intermolecular contacts are observed between the catalyst and different proton signals of SDS (αCH_2, βCH_2, and main chain CH_2), confirming that the catalyst is positioned on the micelle surface in the presence of SDS micelles.

In particular, catalysts H3/H8 and H20/H31 interact selectively with SDS αCH_2 and H4/H7, whereas H1/H10, H18/H29, H15, H26, H21/H3, and H12/H23 interact with SDS α and βCH_2, as reported in Figure 7b. The main chain CH_2 of SDS interacts with all of the catalyst protons, indicating a degree of movement freedom. Paramagnetic probes and NOE results are consistent and allowed us to establish the average relative disposition of the [Ir(ppy)$_2$bpy]PF$_6$/SDS system, as reported in Figure 8.

https://doi.org/10.1021/acsorginorgau.1c00028
ACS Org. Inorg. Au 2022, 2, 66−74

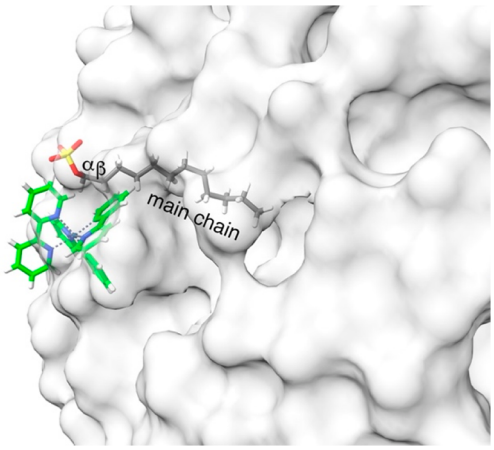

Figure 8. Graphic representation of $[Ir(ppy)_2bpy]PF_6$ bound with SDS micelle. Catalyst atoms are reported with the following color codes: carbon, green; hydrogen, white; nitrogen, blue. The micelle is reported as a gray surface. For the sake of clarity, only one SDS molecule is shown (color code: carbon, gray; hydrogen, white; oxygen, red; sulfur, yellow).

In this model the 2,2′-bipyridine moiety is positioned mostly outside, whereas the 2-phenylpyridinates are located inside the micelle. Overall, the obtained experimental data strongly suggest that, for an optimal catalytic efficiency, the photocatalyst must be positioned on the micelles' surface and almost free to move inside and outside the micelles. Consistently, the latter conditions could be enabled by micellar systems with a reverse polarity with the respect to the photocatalyst as in the case of $[Ir(ppy)_2bpy]PF_6$ and SDS.

CONCLUSION

In conclusion, optimum photomicellar catalytic conditions for the synthesis of amides starting from readily available *N*-methyl-*N*-alkyl aromatic amines and both aliphatic and aromatic isocyanides have been developed. The substrate scope is broad with a good functional group tolerance as further highlighted in late-stage functionalization of drugs and natural compounds. Moreover, this transformation can be performed under sunlight irradiation without any decrease in the yield. The possibility to recycle the micellar solvent system, as shown for up to four cycles, while preserving conversion and yields of the amide target compounds, further supports the greenness of the developed conditions. Furthermore, in order to provide information at the atomic level about the interactions between the photocatalyst and the micelles as well as the photocatalyst localization with respect to the latter, solution 1D and 2D NMR experiments were performed in the presence of paramagnetic probes. To our knowledge, this represents the first application of such probes to the characterization of a (photo)micellar reaction environment. Such studies revealed a reverse polarity principle, according to which a negatively charged surfactant such as SDS could provide the localization of a positively charged photocatalyst on the micelles' surface, while a cation surfactant such as CTAC will cause a burying of the photocatalyst deeply into the micelles, probably preventing its interaction with light. We are confident that the rationalization of the optimum photocatalyst/surfactant pairing could drive the exploration and the optimization of future photomicellar-catalyzed reactions, thus promoting the merging of these intrinsically green chemical approaches underlying the flourishing of *in water* photoredox catalytic transformations.

EXPERIMENTAL SECTION

General Synthetic Methods

Commercially available reagents and solvents were used without further purification. When necessary, the reactions were performed in oven-dried glassware under a positive pressure of dry nitrogen. Photochemical reactions were carried out using a PhotoRedOx Box (EvoluChemTM) with a 30 W blue LED (EvoluChemTM, model: HCK1012-01-008, wavelength 450 nm, LED: CREE XPE). A holder suitable for 4 mL scintillation vials (45 × 14.7 mm) was fitted with a Schlenk flask: this allows a fixed sample placement distance from the light source. All NMR spectra were obtained with a Bruker Avance NEO 400 or 700 MHz instrument. Experiments for structure elucidation were performed in $CDCl_3$ at 25 °C with a RT-DR-BF/1H-5 mm-OZ SmartProbe. High-resolution ESI-MS spectra were obtained on a Thermo LTQ Orbitrap XL mass spectrometer. The spectra were recorded by infusion into the ESI source using MeOH as the solvent. Chemical shifts (δ) are reported in parts per million (ppm) relative to the residual solvent peak. Column chromatography was performed on silica gel (70−230 mesh ASTM) using the reported eluents. Thin layer chromatography (TLC) was carried out on 5 × 20 cm plates with a layer thickness of 0.25 mm (silica gel 60 F254) to monitor the reaction using UV as the revelation methods.

General Procedure for the Preparation of Compounds 3−20 (Method A)

To a 4 mL colorless glass vial equipped with a magnetic stir bar were added the isocyanide (0.3 mmol, 1 equiv), the photocatalyst $[Ir(ppy)_2bpy]PF_6$ (0.003 mmol, 1% mol), and the aniline derivative (0.6 mmol, 2 equiv). Then 2 mL of the micellar solution (2% weight/volume concentration) (0.15 M) was added into the reaction vial, and the resulting mixture was stirred in an open flask in a PhotoRedOx Box, under 30 W blue LED irradiation, at room temperature for 48 h. After the completion of the reaction, as monitored by TLC (hexane/EtOAc 7:3 and 5:5), the reaction mixture was extracted with EtOAc (3×), the collected organic layers were washed with brine (1×), dried over dry Na_2SO_4, filtered, and evaporated to dryness to give a reaction crude which was purified as specified for each compound.

2-(Methyl(phenyl)amino)-*N*-(tosylmethyl)acetamide 3[21]

The title compound **3** was prepared following the general procedure method A. The crude material was purified by trituration with hexane/EtOAc (2:1) or column chromatography (hexane/EtOAc 8:2 to 5:5). Yield: 74.8 mg, 75%; white amorphous solid; R_f = 0.4 (TLC hexane/EtOAc 5:5). ^{1}H NMR (400 MHz, $CDCl_3$): δ 7.72 (d, J = 8.3 Hz, 2H), 7.37−7.26 (m, 5H), 6.89 (t, J = 7.3 Hz, 1H), 6.68 (d, J = 7.9 Hz, 2H), 4.69 (d, J = 6.9 Hz, 2H), 3.75 (s, 2H), 2.99 (s, 3H), 2.46 (s, 3H). ^{13}C NMR (100 MHz, $CDCl_3$): δ 170.3, 149.0, 145.6, 133.8, 130.0, 129.5, 128.8, 119.3, 113.4, 59.8, 58.6, 40.1, 21.8. HRMS−ESI: m/z $[M + H]^+$ calcd for $C_{17}H_{21}N_2O_3S^+$ = 333.1267; found = 333.1279.

2-(Methyl(phenyl)amino)-*N*-pentylacetamide 4[32]

The title compound **4** was prepared following the general procedure method A. The crude material was purified by column chromatography (hexane/EtOAc 8:2 to 6:4). Yield: 47.1 mg, 67%; colorless oil; R_f = 0.4 (TLC hexane/EtOAc 6:4). ^{1}H NMR (400 MHz, $CDCl_3$): δ 7.31−7.23 (m, 2H), 6.84 (t, J = 7.3 Hz, 1H), 6.77−6−70 (m, 2H), 6.56 (brs, 1H), 3.85 (s, 2H), 3.27 (q, J = 9.4 Hz, 2H), 3.00 (s, 3H), 1.49−1.41 (m, 2H), 1.34−1.16 (m, 4H), 0.85 (t, J = 7.2 Hz, 3H). ^{13}C NMR (100 MHz, $CDCl_3$): δ 170.2, 149.3, 129.4, 118.6, 113.1, 59.0, 39.7, 39.2, 29.3, 29.0, 22.3, 14.0. HRMS−ESI: m/z $[M + H]^+$ calcd for $C_{14}H_{23}N_2O^+$ = 235.1805; found = 235.1808.

Methyl *N*-Methyl-*N*-phenylglycylglycinate 5[21]

The title compound **5** was prepared following the general procedure method A. The crude material was purified by column chromatography (hexane/EtOAc 8:2 to 6:4). Yield: 48.2 mg, 68%; colorless oil;

https://doi.org/10.1021/acsorginorgau.1c00028
ACS Org. Inorg. Au 2022, 2, 66−74

R_f = 0.4 (TLC hexane/EtOAc 6:4). ^{1}H NMR (400 MHz, $CDCl_3$): δ 7.31−7.25 (m, 2H), 7.05 (brs, 1H), 6.85 (t, J = 7.3 Hz, 1H), 6.81−6.75 (m, 2H), 4.07 (d, J = 5.8 Hz, 2H), 3.91 (s, 2H), 3.73 (s, 3H), 3.04 (s, 3H). ^{13}C NMR (100 MHz, $CDCl_3$): δ 171.1, 170.0, 149.3, 129.4, 118.9, 113.4, 58.8, 52.4, 40.8, 39.8. HRMS−ESI: m/z [M + H]$^+$ calcd for $C_{12}H_{17}N_2O_3^+$ = 237.1234; found = 237.1243.

N-Benzyl-2-(methyl(phenyl)amino)acetamide 6[21]

The title compound **6** was prepared following the general procedure method A. The crude material was purified by column chromatography (hexane/EtOAc 8:2 to 6:4). Yield: 57.2 mg, 75%; colorless oil; R_f = 0.4 (TLC hexane/EtOAc 6:4). ^{1}H NMR (400 MHz, $CDCl_3$): δ 7.32−7.23 (m, 5H), 7.22−7.17 (m, 2H), 6.91 (brs, 1H, NH), 6.84 (t, J = 7.3 Hz, 1H), 6.77−6.71 (m, 2H), 4.49 (d, J = 6.0 Hz, 2H), 3.92 (s, 2H), 3.00 (s, 3H). ^{13}C NMR (100 MHz, $CDCl_3$): δ 170.4, 149.3, 138.0, 129.4, 128.7, 127.5, 127.5, 118.8, 113.3, 59.0, 43.1, 39.9. HRMS−ESI: m/z [M + H]$^+$ calcd for $C_{16}H_{19}N_2O^+$ = 255.1492; found = 255.1504.

N-Cyclohexyl-2-(methyl(phenyl)amino)acetamide 7[21]

The title compound **7** was prepared following the general procedure method A. The crude material was purified by column chromatography (hexane/EtOAc 8:2 to 6:4). Yield: 40.6 mg, 55%; colorless oil; R_f = 0.4 (TLC hexane/EtOAc 6:4). ^{1}H NMR (400 MHz, $CDCl_3$): δ 7.31−7.23 (m, 2H), 6.84 (t, J = 7.3 Hz, 1H), 6.77−6−71 (m, 2H), 6.45 (brs, 1H), 3.86−3−81 (m, 3H), 2.99 (s, 3H), 1.90−1.80 (m, 2H), 1.72−1.53 (m, 4H), 1.40−1.34 (m, 2H), 1.17−0.99 (m, 2H). ^{13}C NMR (100 MHz, $CDCl_3$): δ 169.3, 150.1, 129.4, 118.7, 113.3, 59.2, 47.8, 39.7, 33.0, 25.4, 24.8. HRMS−ESI: m/z [M + H]$^+$ calcd for $C_{15}H_{23}N_2O^+$ = 247.1805; found = 247.1815.

N-([1,1′-Biphenyl]-4-yl)-2-(methyl(phenyl)amino)-acetamide 8

The title compound **8** was prepared following the general procedure method A (with 3 equiv of *N,N*-dimethylaniline for 72 h). The crude material was purified by column chromatography (hexane/EtOAc 8:2 to 6:4). Yield: 75.9 mg, 80%; pale-brown solid; R_f = 0.4 (TLC hexane/EtOAc 6:4). ^{1}H NMR (400 MHz, $CDCl_3$): δ 8.47 (brs, 1H, NH), 7.63−7.58 (m, 2H), 7.58−7.53 (m, 4H), 7.45−7.40 (m,2H), 7.36−7.29 (m, 2H), 6.91 (t, J = 7.3 Hz, 1H), 6.88−6.84 (m, 2H), 3.98 (s, 4H), 3.10 (s, 3H). ^{13}C NMR (100 MHz, $CDCl_3$): δ 168.8, 149.5, 140.5, 137.5, 136.5, 129.6, 128.8, 127.6, 127.2, 126.9, 120.2, 119.5, 113.8, 60.1, 40.1. HRMS−ESI: m/z [M + H]$^+$ calcd for $C_{21}H_{21}N_2O^+$ = 317.1648; found = 317.1662.

N-(4-Chlorophenyl)-2-(methyl(phenyl)amino)acetamide 9[33]

The title compound **9** was prepared following the general procedure method A. The crude material was purified by column chromatography (hexane/EtOAc 8:2 to 6:4). Yield: 67.6 mg, 82%; whitish solid; R_f = 0.4 (TLC hexane/EtOAc 6:4). ^{1}H NMR (400 MHz, $CDCl_3$): δ 8.43 (s, 1H), 7.52−7.44 (m, 2H), 7.35−7.26 (m, 4H), 6.91 (t, J = 7.3 Hz, 1H), 6.85−6.80 (m, 2H), 3.95 (s, 2H), 3.08 (s, 3H). ^{13}C NMR (100 MHz, $CDCl_3$): δ 168.9, 149.6, 135.9, 129.4, 129.7, 129.2, 121.3, 119.7, 113.9, 60.2, 40.3. HRMS−ESI: m/z [M + H]$^+$ calcd for $C_{15}H_{16}ClN_2O^+$ = 275.0946; found = 275.0955.

N-(3,4-Dimethoxyphenyl)-2-(methyl(phenyl)amino)-acetamide 10

The title compound **10** was prepared following the general procedure method A (with 3 equiv of *N,N*-dimethylaniline and 2% of photocatalyst for 72 h). The crude material was purified by column chromatography (hexane/EtOAc 8:2 to 6:4). Yield: 76.6 mg, 85%; yellow solid; R_f = 0.4 (TLC hexane/EtOAc 6:4). ^{1}H NMR (400 MHz, $CDCl_3$): δ 8.33 (s, 1H), 7.35−7.28 (m, 3H), 6.93−6.87 (m, 2H), 6.86−6.82 (m, 2H), 6.79 (d, J = 8.6 Hz, 1H), 3.95 (s, 2H), 3.89 (s, 3H), 3.85 (s, 3H), 3.08 (s, 3H). ^{13}C NMR (100 MHz, $CDCl_3$): δ 168.6, 149.7, 149.2, 146.2, 131.0, 129.6, 119.5, 113.9, 112.0, 111.4, 104.9, 60.2, 56.2, 56.1, 40.2. HRMS−ESI: m/z [M + H]$^+$ calcd for $C_{17}H_{21}N_2O_3^+$ = 301.1547; found = 301.1556.

N-(2,3-Dihydrobenzo[*b*][1,4]dioxin-6-yl)-2-(methyl-(phenyl)amino)acetamide 11

The title compound **11** was prepared following the general procedure method A (with 3 equiv of *N,N*-dimethylaniline and 2% of photocatalyst for 72 h). The crude material was purified by column chromatography (hexane/EtOAc 8:2 to 6:4). Yield: 78.8 mg, 88%; yellow solid; R_f = 0.4 (TLC hexane/EtOAc 6:4). ^{1}H NMR (400 MHz, $CDCl_3$): δ 8.26 (s, 1H), 7.33−7.27 (m, 2H), 7.17 (d, J = 2.5 Hz, 1H), 6.92−6.85 (m, 2H), 6.84−6.76 (m, 3H), 4.25−4.20 (m, 4H), 3.93 (s, 2H), 3.06 (s, 3H). ^{13}C NMR (100 MHz, $CDCl_3$): δ 168.5, 149.6, 143.6, 140.8, 131.0, 129.6, 119.4, 117.3, 113.8, 113.7, 109.9, 64.5, 64.4, 60.0, 40.2. HRMS−ESI: m/z [M + H]$^+$ calcd for $C_{17}H_{19}N_2O_3^+$ = 299.1390; found = 299.1399.

2-(Methyl(*p*-tolyl)amino)-*N*-(tosylmethyl)acetamide 12[21]

The title compound **12** was prepared following the general procedure method A. The crude material was purified by column chromatography (hexane/EtOAc 8:2 to 6:4). Yield: 81.0 mg, 78%; whitish solid; R_f = 0.4 (TLC hexane/EtOAc 5:5). ^{1}H NMR (700 MHz, $CDCl_3$): δ 7.75−7.70 (m, 2H), 7.38 (s, 1H), 7.36−7.32 (m, 2H), 7.12−7.07 (m, 2H), 6.65−6.55 (m, 2H), 4.69 (d, J = 6.8 Hz, 2H), 3.70 (s, 2H), 2.95 (s, 3H), 2.46 (s, 3H), 2.29 (s, 3H). ^{13}C NMR (100 MHz, $CDCl_3$): δ 170.5, 147.0, 145.6, 133.8, 130.0, 129.9, 128.9, 128.8, 113.8, 59.8, 58.9, 40.4, 21.8, 20.3. HRMS−ESI: m/z [M + H]$^+$ calcd for $C_{18}H_{23}N_2O_3S^+$ = 347.1424; found = 347.1435.

2-(Methyl(*m*-tolyl)amino)-*N*-(tosylmethyl)acetamide 13[21]

The title compound **13** was prepared following the general procedure method A. The crude material was purified by column chromatography (hexane/EtOAc 8:2 to 6:4). Yield: 79.0 mg, 76%; whitish solid; R_f = 0.4 (TLC hexane/EtOAc 5:5). ^{1}H NMR (700 MHz, $CDCl_3$): δ 7.75−7.70 (m, 2H), 7.36−7.29 (m, 3H), 7.17 (t, J = 7.8 Hz, 1H), 6.71 (d, J = 7.1 Hz, 1H), 6.52 (s, 1H), 6.48 (d, J = 8.1 Hz, 1H), 4.68 (d, J = 6.8 Hz, 2H), 3.74 (s, 2H), 2.97 (s, 3H), 2.45 (s, 3H), 2.34 (s, 3H). ^{13}C NMR (100 MHz, $CDCl_3$): δ 170.4, 149.1, 145.5, 139.4, 133.8, 130.0, 129.3, 128.8, 120.2, 114.2, 110.6, 59.9, 58.6, 40.1, 21.8, 21.8. HRMS−ESI: m/z [M + H]$^+$ calcd for $C_{18}H_{23}N_2O_3S^+$ = 347.1424; found = 347.1437.

-((4-Bromophenyl)(methyl)amino)-*N*-(tosylmethyl)-acetamide 14[34]

The title compound **14** was prepared following the general procedure method A. The crude material was purified by column chromatography (hexane/EtOAc 8:2 to 6:4). Yield: 86.4 mg, 70%; whitish solid; R_f = 0.4 (TLC hexane/EtOAc 5:5). ^{1}H NMR (700 MHz, $CDCl_3$): δ 7.76−7.72 (m, 2H), 7.40−7.30 (m, 4H), 7.18 (s, 2H), 6.55−6.50 (m, 2H), 4.69 (d, J = 6.8 Hz, 2H), 3.74 (s, 2H), 2.98 (s, 3H), 2.47 (s, 3H). ^{13}C NMR (100 MHz, $CDCl_3$): δ 169.8, 147.9, 145.7, 133.7, 132.2, 130.1, 130.0, 128.8, 128.8, 115.0, 111.5, 59.8, 58.4, 40.2, 21.8. HRMS−ESI: m/z [M + H]$^+$ calcd for $C_{17}H_{20}BrN_2O_3S^+$ = 411.0373; found = 411.0387.

2-((3-Bromophenyl)(methyl)amino)-*N*-(tosylmethyl)-acetamide 15[21]

The title compound **15** was prepared following the general procedure method A. The crude material was purified by trituration with hexane/EtOAc (2:1). Yield: 90.1 mg, 73%; whitish solid; R_f = 0.4 (TLC hexane/EtOAc 5:5). ^{1}H NMR (700 MHz, $CDCl_3$): δ 7.75−7.70 (m, 2H), 7.38−7.33 (m, 2H), 7.17 (t, J = 6.6 Hz, 1H), 7.13 (t, J = 8.1 Hz, 1H), 7.00 (d, J = 7.8 Hz, 1H), 6.82 (s, 1H), 6.57 (dd, J = 8.3, 2.2 Hz, 1H), 4.68 (d, J = 6.8 Hz, 2H), 3.76 (s, 2H), 2.98 (s, 3H), 2.46 (s, 3H). ^{13}C NMR (176 MHz, $CDCl_3$): δ 169.6, 150.2, 145.7, 133.7, 130.7, 130.1, 128.8, 123.7, 122.0, 116.6, 111.9, 59.8, 58.0, 39.9, 21.8. HRMS−ESI: m/z [M + H]$^+$ calcd for $C_{17}H_{20}BrN_2O_3S^+$ = 411.0373; found = 411.0389.

2-((3-Chlorophenyl)(methyl)amino)-*N*-(tosylmethyl)-acetamide 16

The title compound **16** was prepared following the general procedure method A. The crude material was purified by trituration with hexane/EtOAc (2:1). Yield: 80.3 mg, 73%; pale-brown solid; R_f = 0.4

https://doi.org/10.1021/acsorginorgau.1c00028
ACS Org. Inorg. Au 2022, 2, 66−74

(TLC hexane/EtOAc 5:5). ^{1}H NMR (700 MHz, $CDCl_3$): δ 7.75−7.70 (m, 2H), 7.38−7.33 (m, 2H), 7.19 (t, J = 8.1 Hz, 1H), 7.14 (t, J = 6.5 Hz, 1H), 6.86 (dd, J = 7.9, 1.0 Hz, 1H), 6.65 (t, J = 2.0 Hz, 1H), 6.53 (dd, J = 8.4, 2.4 Hz, 1H), 4.69 (d, J = 6.8 Hz, 2H), 3.76 (s, 2H), 2.99 (s, 3H), 2.46 (s, 3H). ^{13}C NMR (176 MHz, $CDCl_3$): δ 169.6, 150.0, 145.7, 135.4, 133.7, 130.5, 130.0, 128.8, 119.1, 113.3, 111.4, 59.8, 58.1, 40.0, 21.8. HRMS−ESI: m/z [M + H]$^+$ calcd for $C_{17}H_{20}ClN_2O_3S^+$ = 367.0878; found = 367.0893.

2-((3,5-Dimethylphenyl)(methyl)amino)-*N*-(tosylmethyl)-acetamide 17[21]

The title compound **17** was prepared following the general procedure method A. The crude material was purified by trituration with hexane/EtOAc (2:1). Yield: 75.7 mg, 70%; whitish solid; R_f = 0.4 (TLC hexane/EtOAc 5:5). ^{1}H NMR (700 MHz, $CDCl_3$): δ 7.74−7.69 (m, 2H), 7.34−7.29 (m, 2H), 6.55 (s, 1H), 6.33 (s, 2H), 4.68 (d, J = 6.9 Hz, 2H), 3.73 (s, 2H), 2.95 (s, 3H), 2.45 (s, 3H), 2.30 (s, 6H). ^{13}C NMR (100 MHz, $CDCl_3$): δ 169.5, 148.2, 144.5, 138.2, 132.9, 128.9, 127.8, 120.2, 110.4, 58.8, 57.6, 39.0, 20.8, 20.7. HRMS−ESI: m/z [M + H]$^+$ calcd for $C_{19}H_{25}N_2O_3S^+$ = 361.1580; found = 361.1592.

2-(Ethyl(phenyl)amino)-*N*-(tosylmethyl)acetamide 18[21]

The title compound **18** was prepared following the general procedure method A. The crude material was purified by column chromatography (hexane/EtOAc 8:2 to 6:4). Yield: 52 mg, 50%; white solid; R_f = 0.4 (TLC hexane/EtOAc 5:5). ^{1}H NMR (400 MHz, $CDCl_3$): δ 7.73−7.68 (m, 2H), 7.36−7.26 (m, 5H), 6.88 (t, J = 7.3 Hz, 1H), 6.70−6.65 (m, 2H), 4.67 (d, J = 6.9 Hz, 2H), 3.75 (s, 2H), 3.43 (q, J = 7.1 Hz, 2H), 2.47 (s, 3H), 1.19 (t, J = 7.1 Hz, 3H). ^{13}C NMR (100 MHz, $CDCl_3$): δ 170.5, 147.4, 145.5, 133.9, 129.9, 129.6, 128.8, 119.0, 113.7, 59.9, 55.4, 46.5, 21.8, 11.5. HRMS−ESI: m/z [M + H]$^+$ calcd for $C_{18}H_{23}N_2O_3S^+$ = 347.4525; found = 347.4534.

(1*R*,4a*R*,4b*R*,10a*R*)-7-Isopropyl-1,4a-dimethyl-*N*-(4-(methyl(2-oxo-2((tosylmethyl)amino)ethyl)amino)-benzyl)-1,2,3,4,4a,4b,5,6,10,10a-decahydrophenanthrene-1-carboxamide 19

The title compound **19** was prepared following the general procedure method A (using 0.15 mmol of isocyanide). The crude material was purified by column chromatography (hexane/EtOAc 8:2 to 5:5). Yield: 30 mg, 31%; white solid; R_f = 0.4 (TLC hexane/EtOAc 5:5). ^{1}H NMR (400 MHz, $CDCl_3$): δ 7.75−7.70 (m, 2H), 7.36−7.31 (m, 2H), 7.20−7.15 (m, 2H), 6.65−6.60 (m, 2H), 5.94 (t, J = 5.0 Hz, 1H), 5.74 (s, 1H), 5.32 (d, J = 4.5 Hz, 1H), 4.68 (d, J = 6.9 Hz, 2H), 4.38 (d, J = 5.6 Hz, 1H), 4.31 (d, J = 5.1 Hz, 1H), 3.74 (s, 2H), 2.98 (s, 3H), 2.46 (s, 3H), 2.21 (s, 1H), 2.10−1.79 (m, 10H), 1.62−1.50 (m, 2H), 1.27−1.22 (m, 5H), 1.00 (dd, J = 6.8, 3.3 Hz, 6H), 0.82 (s, 3H). ^{13}C NMR (100 MHz, $CDCl_3$): δ 178.2, 170.1, 148.4, 145.6, 145.3, 135.6, 133.8, 130.0, 129.4, 129.2, 128.8, 122.4, 120.4, 113.6, 59.9, 58.5, 51.0, 46.4, 45.7, 43.3, 40.1, 38.3, 37.7, 34.9, 34.7, 27.4, 25.4, 22.5, 21.8, 21.4, 20.8, 18.3, 17.1, 14.1. HRMS−ESI: m/z [M + H]$^+$ calcd for $C_{38}H_{52}N_3O_4S^+$ = 646.3673; found = 646.3701.

5-(2,5-Dimethylphenoxy)-2,2-dimethyl-*N*-(4-(methyl-(2-oxo-2-((tosylmethyl)amino)ethyl)amino)benzyl)-pentanamide 20

The title compound **20** was prepared following the general procedure method A (using 0.12 mmol of isocyanide). The crude material was purified by column chromatography (hexane/EtOAc 8:2 to 5:5). Yield: 28.5 mg, 40%; color-less oil; R_f = 0.4 (TLC hexane/EtOAc 5:5). ^{1}H NMR (400 MHz, $CDCl_3$): 7.73−7.68 (m, 2H), 7.36−7.27 (m, 3H), 7.20−7.15 (m, 2H), 6.99 (d, J = 7.4 Hz, 1H), 6.65−6.60 (m, 4H), 5.92 (t, J = 5.0 Hz, 1H), 4.66 (d, J = 6.9 Hz, 2H), 4.36 (d, J = 5.5 Hz, 2H), 3.91 (t, J = 5.7 Hz, 2H), 3.73 (s, 2H), 2.96 (s, 3H), 2.45 (s, 3H), 2.30 (s, 3H), 2.14 (s, 3H), 1.80−1.67 (m, 2H), 1.22 (s, 6H). ^{13}C NMR (100 MHz, $CDCl_3$): δ 177.3, 170.1, 156.9, 148.4, 145.6, 136.5, 133.8, 130.3, 130.0, 129.3, 129.1, 128.8, 123.5, 120.8, 113.6, 112.1, 68.0, 59.9, 58.4, 43.0, 41.9, 40.1, 37.5, 25.6, 25.2, 21.8, 21.4, 15.8. HRMS−ESI: m/z [M + H]$^+$ calcd for $C_{33}H_{44}N_3O_5S^+$ = 594.2996; found = 594.3016.

(1*R*,4a*R*,4b*R*,10a*R*)-*N*-(4-(Dimethylamino)-benzyl)-7-isopropyl-1,4a-dimethyl-1,2,3,4,4a,4b,5,6,10,10a-decahydrophenanthrene-1-carboxamide 21

The title compound **21** was prepared by reacting 4-(dimethylamino)-benzylamine dihydrochloride with abietic acid (1.1 equiv) in the presence of EDC HCl (1.1 equiv), DIPEA (5 equiv), and DMAP (5 mol %) in DCM (0.15 M) at room temperature overnight. The crude material was purified by column chromatography (hexane/EtOAc 90:10 to 85:15). Yield: 131 mg, 20%; amorphous solid; R_f = 0.4 (TLC hexane/EtOAc 8:2). ^{1}H NMR (700 MHz, DMSO-d_6): δ 7.89 (t, J = 5.7 Hz, 1H), 7.05−7.00 (m, 2H), 6.68−6.63 (m, 2H), 5.71 (s, 1H), 5.30 (d, J = 5.1 Hz, 1H), 4.18−4.08 (m, 2H), 2.85 (s, 6H), 2.25−2.16 (m, 1H), 2.10−1.36 (m, 12H), 1.17 (s, 3H), 1.15−1.08 (m, 2H), 0.97 (dd, J = 6.8, 1.5 Hz, 6H), 0.76 (s, 3H). ^{13}C NMR (176 MHz, DMSO-d_6): δ 177.7, 149.9, 144.7, 135.3, 128.4, 128.3, 122.9, 121.2, 112.8, 50.9, 45.8, 45.1, 42.4, 40.8, 38.2, 37.6, 34.7, 34.6, 27.4, 25.3, 22.4, 21.8, 21.2, 18.4, 17.4. HRMS−ESI: m/z [M + H]$^+$ calcd for $C_{29}H_{43}N_2O^+$ = 435.33699; found = 435.3381.

N-(4-(Dimethylamino)-benzyl)-5-(2,5-dimethylphenoxy)-2,2-dimethylpentanamide 22

The title compound **22** was prepared by reacting 4-(dimethylamino)-benzylamine dihydrochloride with gemfibrozil (1.1 equiv) in the presence of EDC HCl (1.1 equiv), DIPEA (5 equiv), and DMAP (5 mol %) in DMF (0.6 M) at room temperature overnight. The crude material was diluted with brine and the product extracted with ethyl acetate (5×). The organic phase was further washed with brine solution (5×), dried over sodium sulfate, filtered, and evaporated under reduced pressure. The resulting mixture was purified by column chromatography (hexane/EtOAc 90:10 to 80:20). Yield: 93 mg, 13.5%; amorphous solid; R_f = 0.8 (TLC hexane/EtOAc 5:5). ^{1}H NMR (700 MHz, $CDCl_3$): δ 7.17−7.13 (m, 2H), 6.99 (d, J = 7.4 Hz, 1H), 6.73−6.68 (m, 2H), 6.66 (d, J = 7.5 Hz, 1H), 6.61 (s, 1H), 5.80 (brs, 1H, NH), 4.34 (d, J = 5.3 Hz, 2H), 3.91 (t, J = 6.1 Hz, 2H), 2.94 (s, 6H), 2.30 (s, 3H), 2.15 (s, 3H), 1.80−1.73 (m, 2H), 1.72−1.69 (m, 2H), 1.22 (s, 6H). ^{13}C NMR (176 MHz, $CDCl_3$): δ 177.1, 156.9, 136.5, 130.3, 128.9, 123.5, 120.7, 112.0, 68.0, 43.3, 41.9, 37.6, 25.6, 25.1, 21.4, 15.8. HRMS−ESI: m/z [M + H]$^+$ calcd for $C_{24}H_{35}N_2O_2^+$ = 383.5555; found = 383.5572.

NMR Spectroscopy

The samples for NMR spectroscopy were prepared by dissolving the appropriate amount of $[Ir(ppy)_2bpy]PF_6$ in 0.54 mL of CTAC and SDS (either deuterated or not) 2% aqueous solutions and 0.06 mL of ^2H_2O (pH 5.0) to obtain a concentration 1.5 mM of $[Ir(ppy)_2bpy]$-PF_6. NMR experiments were recorded on a Bruker Avance NEO 600 MHz spectrometer equipped with a z-gradient 5 mm triple-resonance probe head. For interaction studies between the micelles and $[Ir(ppy)_2bpy]PF_6$, DQF-COSY,[25,26] TOCSY,[27] and NOESY[28] spectra were recorded in the phase-sensitive mode using the method from States.[35] TOCSY experiments were acquired with a mixing time of 80 ms and a data block size of 4096 addresses in t_2 and 256 equidistant t_1 values. NOESY experiments were run with a mixing time of 500 ms. The proton, DQF-COSY, TOCSY, and NOESY spectra were processed and analyzed with the Bruker TOPSPIN 4.1.1 software packages.

■ ASSOCIATED CONTENT

Supporting Information

The Supporting Information is available free of charge at https://pubs.acs.org/doi/10.1021/acsorginorgau.1c00028.

Copies of ^{1}H and ^{13}C NMR spectra (PDF)

https://doi.org/10.1021/acsorginorgau.1c00028
ACS Org. Inorg. Au 2022, 2, 66−74

AUTHOR INFORMATION

Corresponding Authors

Alfonso Carotenuto − *Department of Pharmacy, University of Naples Federico II, 80131 Napoli, Italy;* orcid.org/0000-0001-7532-5449; Email: alfonso.carotenuto@unina.it

Diego Brancaccio − *Department of Pharmacy, University of Naples Federico II, 80131 Napoli, Italy;* Email: diego.brancaccio@unina.it

Mariateresa Giustiniano − *Department of Pharmacy, University of Naples Federico II, 80131 Napoli, Italy;* orcid.org/0000-0002-6856-414X; Email: mariateresa.giustiniano@unina.it

Authors

Rolando Cannalire − *Department of Pharmacy, University of Naples Federico II, 80131 Napoli, Italy*

Federica Santoro − *Department of Pharmacy, University of Naples Federico II, 80131 Napoli, Italy*

Camilla Russo − *Department of Pharmacy, University of Naples Federico II, 80131 Napoli, Italy;* orcid.org/0000-0001-6303-3430

Giulia Graziani − *Department of Pharmacy, University of Naples Federico II, 80131 Napoli, Italy*

Gian Cesare Tron − *Department of Drug Science, University of Piemonte Orientale, 28100 Novara, Italy;* orcid.org/0000-0002-2394-400X

Complete contact information is available at: https://pubs.acs.org/10.1021/acsorginorgau.1c00028

Author Contributions

§R.C. and F.S. contributed equally.

Notes

The authors declare no competing financial interest.

ACKNOWLEDGMENTS

Financial support from Universitá degli Studi di Napoli "Federico II" and Universitá del Piemonte Orientale, Novara, Italy, is acknowledged. M.G. acknowledges PROGEMA (ARS01_X00432, PON R&I 2014-2020). R.C. acknowledges MIUR-Ministero dell'Istruzione, dell'Università e della Ricerca (Italian Ministry of Education, University and Research), PON R&I 2014-2020-AIM (Attraction and International Mobility), project AIM1873131 - Num. Attività 2 - Linea 2.1.

ABBREVIATIONS

PQS, polyethylene glycol ubiquinol succinate; TPGS, tocopheryl polyethylene glycol succinate; SDS, sodium dodecyl sulfate; CTAC, cetyltrimethylammonium chloride; EtOAC, ethyl acetate

REFERENCES

(1) Narayan, S.; Muldoon, J.; Finn, M. G.; Fokin, V. V.; Kolb, H. C.; Sharpless, K. B. On Water": Unique Reactivity of Organic Compounds in Aqueous Suspension. *Angew. Chem., Int. Ed.* **2005**, *44*, 3275−3279.

(2) Hayashi, Y. In Water or in the Presence of Water? *Angew. Chem., Int. Ed.* **2006**, *45*, 8103−8104.

(3) Blackmond, D. G.; Armstrong, A.; Coombe, V.; Wells, A. Water in Organocatalytic Processes: Debunking the Myths. *Angew. Chem., Int. Ed.* **2007**, *46*, 3798−3800.

(4) Chanda, A.; Fokin, V. V. Organic Synthesis "On Water. *Chem. Rev.* **2009**, *109*, 725−748.

(5) Lipshutz, B. H. When Does Organic Chemistry Follow Nature's Lead and "Make the Switch"? *J. Org. Chem.* **2017**, *82*, 2806−2816.

(6) Lipshutz, B. H.; Ghorai, S.; Cortes-Clerget, M. The Hydrophobic Effect Applied to Organic Synthesis: Recent Synthetic Chemistry "in Water. *Chem. - Eur. J.* **2018**, *24*, 6672−6695.

(7) La Sorella, G.; Strukul, G.; Scarso, A. Recent Advances in Catalysis in Micellar Media. *Green Chem.* **2015**, *17*, 644−683.

(8) Sheldon, R. A. Metrics of Green Chemistry and Sustainability: Past, Present, and Future. *ACS Sustainable Chem. Eng.* **2018**, *6*, 32−48.

(9) Handa, S.; Wang, Y.; Gallou, F.; Lipshutz, B. H. Sustainable Fe-Ppm Pd Nanoparticle Catalysis of Suzuki-Miyaura Cross-Couplings in Water. *Science* **2015**, *349* (6252), 1087−1091.

(10) Bu, M. J.; Lu, G. P.; Jiang, J.; Cai, C. Merging Visible-Light Photoredox and Micellar Catalysis: Arylation Reactions with Anilines Nitrosated in Situ. *Catal. Sci. Technol.* **2018**, *8*, 3728−3732.

(11) Giedyk, M.; Narobe, R.; Weiß, S.; Touraud, D.; Kunz, W.; König, B. Photocatalytic Activation of Alkyl Chlorides by Assembly-Promoted Single Electron Transfer in Microheterogeneous Solutions. *Nat. Catal.* **2020**, *3*, 40−47.

(12) Santos, M. S.; Cybularczyk-Cecotka, M.; König, B.; Giedyk, M. Minisci C-H Alkylation of Heteroarenes Enabled by Dual Photoredox/Bromide Catalysis in Micellar Solutions. *Chem. - Eur. J.* **2020**, *26*, 15323−15329.

(13) Jana, S.; Verma, A.; Kadu, R.; Kumar, S. Visible-Light-Induced Oxidant and Metal-Free Dehydrogenative Cascade Trifluoromethylation and Oxidation of 1,6-Enynes with Water. *Chem. Sci.* **2017**, *8*, 6633−6644.

(14) Pelliccia, S.; Alfano, A. I.; Luciano, P.; Novellino, E.; Massarotti, A.; Tron, G. C.; Ravelli, D.; Giustiniano, M. Photocatalytic Isocyanide-Based Multicomponent Domino Cascade toward the Stereoselective Formation of Iminofurans. *J. Org. Chem.* **2020**, *85*, 1981−1990.

(15) Zou, Y.-Q.; Guo, W.; Liu, F.-L.; Lu, L.-Q.; Chen, J.-R.; Xiao, W.-J. Visible-Light-Induced Photocatalytic Formyloxylation Reactions of 3-Bromooxindoles with Water and DMF: The Scope and Mechanism. *Green Chem.* **2014**, *16*, 3787−3795.

(16) Bu, M. J.; Cai, C.; Gallou, F.; Lipshutz, B. H. PQS-Enabled Visible-Light Iridium Photoredox Catalysis in Water at Room Temperature. *Green Chem.* **2018**, *20*, 1233−1237.

(17) Ramamurthy, V. Micellar Control of Photochemical Reactions. *Proc. Indian Acad. Sci. - Chem. Sci.* **1984**, *93*, 635−646.

(18) Fendler, J. H. Microemulsions, Micelles, and Vesicles as Media for Membrane Mimetic Photochemistry. *J. Phys. Chem.* **1980**, *84*, 1485−1491.

(19) Cannalire, R.; Amato, J.; Summa, V.; Novellino, E.; Tron, G. C.; Giustiniano, M. Visible-Light Photocatalytic Functionalization of Isocyanides for the Synthesis of Secondary Amides and Ketene Aminals. *J. Org. Chem.* **2020**, *85*, 14077−14086.

(20) Russo, C.; Cannalire, R.; Luciano, P.; Brunelli, F.; Tron, G.; Giustiniano, M. Visible-Light Photocatalytic Ugi/Aza-Wittig Cascade Towards 2-Aminomethyl-1,3,4-Oxadiazole Derivatives. *Synthesis* **2021**, DOI: 10.1055/a-1543-3924.

(21) Rueping, M.; Vila, C. Visible Light Photoredox-Catalyzed Multicomponent Reactions. *Org. Lett.* **2013**, *15*, 2092−2095.

(22) Rueping, M.; Vila, C.; Bootwicha, T. Continuous Flow Organocatalytic C-H Functionalization and Cross-Dehydrogenative Coupling Reactions: Visible Light Organophotocatalysis for Multicomponent Reactions and C-C, C-P Bond Formations. *ACS Catal.* **2013**, *3*, 1676−1680.

(23) Schönhoff, M. NMR Studies of Sorption and Adsorption Phenomena in Colloidal Systems. *Curr. Opin. Colloid Interface Sci.* **2013**, *18*, 201−213.

(24) Schneider, G. E.; Bolink, H. J.; Constable, E. C.; Ertl, C. D.; Housecroft, C. E.; Pertegàs, A.; Zampese, J. A.; Kanitz, A.; Kessler, F.; Meier, S. B. Chloride Ion Impact on Materials for Light-Emitting Electrochemical Cells. *Dalt. Trans.* **2014**, *43*, 1961−1964.

(25) Piantini, U.; Sorensen, O. W.; Ernst, R. R. Multiple Quantum Filters for Elucidating NMR Coupling Networks. *J. Am. Chem. Soc.* **1982**, *104*, 6800−6801.
(26) Marion, D.; Wüthrich, K. Application of Phase Sensitive Two-Dimensional Correlated Spectroscopy (COSY) for Measurements of 1H-1H Spin-Spin Coupling Constants in Proteins. *Biochem. Biophys. Res. Commun.* **1983**, *113*, 967−974.
(27) Braunschweiler, L.; Ernst, R. R. Coherence Transfer by Isotropic Mixing: Application to Proton Correlation Spectroscopy. *J. Magn. Reson.* **1983**, *53*, 521−528.
(28) Jeener, J.; Meier, B. H.; Bachmann, P.; Ernst, R. R. Investigation of Exchange Processes by Two-dimensional NMR Spectroscopy. *J. Chem. Phys.* **1979**, *71*, 4546.
(29) Saviello, M. R.; Malfi, S.; Campiglia, P.; Cavalli, A.; Grieco, P.; Novellino, E.; Carotenuto, A. New Insight into the Mechanism of Action of the Temporin Antimicrobial Peptides. *Biochemistry* **2010**, *49*, 1477−1485.
(30) Brown, L. R.; Bösch, C.; Wüthrich, K. Location and Orientation Relative to the Micelle Surface for Glucagon in Mixed Micelles with Dodecylphosphocholine EPR and NMR Studies. *Biochim. Biophys. Acta, Biomembr.* **1981**, *642*, 296−312.
(31) Lindberg, M.; Jarvet, J.; Langel, U.; Gräslund, A. Secondary Structure and Position of the Cell-Penetrating Peptide Transportan in SDS Micelles As Determined by NMR. *Biochemistry* **2001**, *40*, 3141−3149.
(32) Guerrero, I.; San Segundo, M.; Correa, A. Iron-Catalyzed C(Sp3)-H Functionalization of N,N-Dimethylanilines with Isocyanides. *Chem. Commun.* **2018**, *54*, 1627−1630.
(33) Zhou, H.; Lu, P.; Gu, X.; Li, P. Visible-Light-Mediated Nucleophilic Addition of an α-Aminoalkyl Radical to Isocyanate or Isothiocyanate. *Org. Lett.* **2013**, *15*, 5646−5649.
(34) Ye, X.; Xie, C.; Huang, R.; Liu, J. Direct Synthesis of α-Amino from N-Alkyl Amines by the Copper-Catalyzed Ugi-Type Reaction. *Synlett* **2012**, *23*, 409−412.
(35) States, D. J.; Haberkorn, R. A.; Ruben, D. J. A 2D Nuclear Overhauser Expt. with Pure Absorption Phase in Four Quadrants. *J. Magn. Reson.* **1982**, *48*, 286−292.

https://doi.org/10.1021/acsorginorgau.1c00028
ACS Org. Inorg. Au 2022, 2, 66−74